Covid-19 diagnosis and clinical symptom expression levels in a deep learning model

Minh-Dat Le Chon [a,b,1,*], Thai-Ngoc Nguyen [c,2]

[a] Ho Chi Minh University of Technology, 268 Ly Thuong Kiet, Ward 14, District 10, Ho Chi Minh City; Postcode: 700000, Viet Nam
[b] VNU-Ho Chi Minh University of Science, 227 D. Nguyen Van Cu, Ward 4, District 5, Ho Chi Minh City; Postcode: 700000, Viet Nam
[c] Ho Chi Minh City University of Medicine and Pharmacy, 217 Hong Bang, Ward 11, District 5, Ho Chi Minh City; Postcode: 700000, Viet Nam
[1] dat.lemindast@hcmut.edu.vn*; [2] thaingoc1401@gmail.com
* Corresponding Author

Received 14 February 2022; accepted 10 March 2022; published 14 March 2022

ABSTRACT

In December 2019, a new strain of virus called COVID-19 (previously designated as 2019-nCoV) caused the first detected outbreak in Wuhan City, Hubei Province, China and since then spread globally. Viruses can cause several types of damage to the respiratory tract, including Tracheitis; Bronchitis; Pneumonia. It is difficult to distinguish coronavirus pneumonia from some other microbiological causes through X-ray images. However, it can be distinguished from a normal person by chest X-ray and CT-Scan, along with clinical judgment through actual symptoms. The following article provides the process and setup of an analytical machine learning model and provides some clinical comparisons between the effectiveness of the machine learning model and the level of clinical symptomatology of a statistical sample. Medical records of some patients in Ho Chi Minh City, Vietnam.

KEYWORDS
Covid-19 diagnosis
Deep learning
VGG-16
X-ray images

1. Introduction

A series of pneumonia cases of unknown etiology occurred in December 2019, in Wuhan, Hubei province, China. On December 31, 2019, 27 unexplained cases of pneumonia were identified and found to be associated with so-called "wet markets" which sell fresh meat and seafood from a variety of animals including bats and pangolins. The pneumonia was found to be caused by a virus identified as" severe acute respiratory syndrome coronavirus 2" (SARS-CoV-2), with the associated disease subsequently termed coronavirus disease 2019 (COVID-19) [1].

Coronaviruses are enveloped, positive single-stranded large RNA viruses that infect humans, but also a wide range of animals. Coronaviruses were first described in 1966 by Tyrell and Bynoe, who cultivated the viruses from patients with common colds 2. Based on their morphology as spherical virions with a core-shell and surface projections resembling a solar corona, they were termed coronaviruses (Latin: corona = crown). Four subfamilies, namely alpha-, beta-, gamma- and delta-coronaviruses exist. While alpha- and beta-coronaviruses apparently originate from mammals, in particular from bats, gamma- and delta-viruses originate from pigs and birds. The genome size varies between 26 kb and 32 kb. Among the seven subtypes of coronaviruses that can infect humans, the beta-coronaviruses may cause severe disease and fatalities, whereas alpha-coronaviruses cause asymptomatic or mildly symptomatic infections. SARS-CoV-2 belongs to the B lineage of the beta-coronaviruses and is closely related to the SARS-CoV virus. The major four structural genes encode the nucleocapsid protein (N), the spike protein (S), a small membrane protein (SM) and the membrane glycoprotein (M) with an additional membrane glycoprotein (HE) occurring in the HCoV-OC43 and HKU1 beta-coronaviruses.

SARS-CoV-2 is 96% identical at the whole-genome level to a bat coronavirus [2]. Disease diagnosis is a critical component of medical imaging in today's society. Medical imaging is commonly referred to as process and referred to as the process and practice of creating visual representations of a body's interior, which is employed in clinical evaluation and for training and medical simulation. Medical imaging uses x-

rays and scans to examine the disease, too. Artificial intelligence and radiology offer a better-than-human vision for medical imaging purposes. Machine learning (ML) is an application of artificial intelligence (AI) in which a system can be constructed and improved without requiring constant human intervention. Developing computer applications that can access and manipulate data, focuses on data development. Machine learning approaches are increasingly utilized in diagnosis, prognosis, and risk assessment to use images. This chapter highlights new rules for imaging research and the results of which four issues that affect machine learning are discussed, including standardization of imagery protocols, diagnosing pathology changes, acquiring insight into images, and finally grasping the significance of test results[3]. The clinical signs show that the first 3 signs are all signs of other diseases such as pneumonia, clinically. This is shown in the Table 1. We are very difficult to identify.

Table 1. The rate of occurrence of clinical symptoms of COVID-19 patients. (Ho Chi Minh City, 2020)

Characteristics	Value (n=31)	Ratio (%)
Dry cough	24	77.4
Fever	15	48.4
Coughing phlegm	12	38.7
Sore throat	7	22.6
Headache	6	19.4
Diarrhea	5	16.1
Muscle pain	3	9.7
Shortness of breath	2	6.5
Runny nose	2	6.5

HRCT Check: CT scan identifies structures and abnormalities inside the chest much better than x-rays. Traditional CT scans provide cross-sectional images of the chest with 10 mm thick slices. Advantages of widely adopted CT Cons are motion noise and limited display in 10 mm thick slices. Chest CT is usually performed at maximal inspiration. Pulmonary ventilation during imaging helps to provide the best image of the lung parenchyma, airways, vascular system, and abnormalities such as a tumor, air-fluid leak, fibrosis. Out of 200 scanned patients with clinical complaints and suspicion, positive HRCT chest findings were seen in 196 patients, showing clinical-radiological correlation and an accuracy of 98% [4]. From the above results, we can see that imaging plays a very important role in identifying lung damage caused by covid. When the clinical symptoms do not assess the condition of the lesion. This is shown in the Fig. 1.

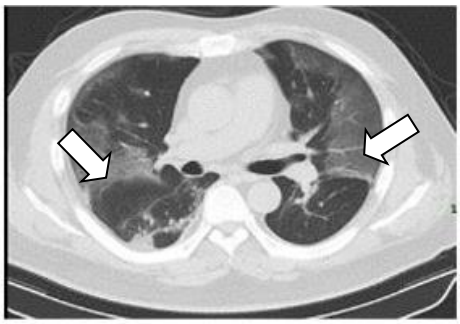

Fig. 1. Opaque-glass opacities appear with additional thickening of the interlobular septum and in the lobules, creating a crazy-paving image -CT scan.

Chest radiography (X-ray) is one of the most important methods used for the diagnosis of pneumonia worldwide [5]. Chest X-ray is a fast, cheap[6], and common clinical method [7] [8]. The chest X-ray gives the patient a lower radiation dose compared to computed tomography (CT) and magnetic resonance imaging (MRI) [8]. However, making the correct diagnosis from X-ray images requires expert knowledge and experience [6]. It is much more difficult to diagnose using a chest X-ray than other imaging modalities such as CT or MRI [6].

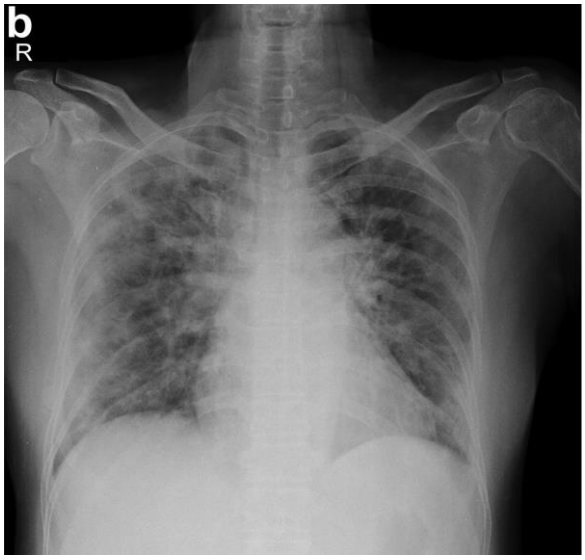

Fig. 2. Faint nodule on straight lung X-ray

The RT-PCR test remains the gold standard for the diagnosis of COVD-19, despite efforts to improve the accuracy of this test technique, there are still cases of false negatives, especially in the early stages. This is shown in the Fig. 2. The early stage of the disease, clinical symptoms, X-rays and CT-Scans are extremely important.

2. Method

2.1. Deep Learning, Machine Learning

Machine learning is one of the fields in the modern computing world. Plenty of research has been undertaken to make machines intelligent. Learning is a natural human behavior that has been made an essential aspect of machines as well. There are various techniques devised for the same. Traditional machine learning algorithms have been applied in many application areas. Researchers have put much effort to improve the accuracy of that machine learning algorithms. Another dimension was given thought which leads to a deep learning concept. Deep learning is a subset of machine learning. So far few applications of deep learning have been explored. This is definitely going to cater to solving issues in several new application domains, sub-domains using deep learning [9].

VGG 16 was proposed by Karen Simonyan and Andrew Zisserman of the Visual Geometry Group Lab of Oxford University in 2014 in the paper "Very deep convolutional networks for large-scale image recognition". This model won 1st and 2nd place on the above categories in the 2014 ILSVRC challenge [10].

2.2. Dataset

In this study, chest X-ray images of 360 COVID-19, 270 normal (healthy) patients chest X-ray images from Kaggle repository called "COVID-19 Patients Lungs X-ray Images", and chest CT Scan images of 270 COVID-19, 180 normal (healthy) patients chest X-ray images also from Kaggle. The data augmentation method was used with scaling factor = 1. All X-rays images were resized to 224 × 224 pixels size in the datasets (The original CT scan image will be programmed to convert to 224 × 224 pixels size). In Fig. 3 and Fig. 4, representative chest X-ray images and chest CT scan images of normal (healthy) and COVID-19 patients are given respectively. The data shown in Table 2 and Table 3.

Table 2. Number of images for each dataset X-rays

Dataset	COVID-19	Normal
X1	120	90
X2	120	90
X3	120	90
Total	360	270

Table 3. Number of images for each dataset CT scan

Dataset	COVID-19	Normal
X1	90	60
X2	90	60
X3	90	60
Total	270	180

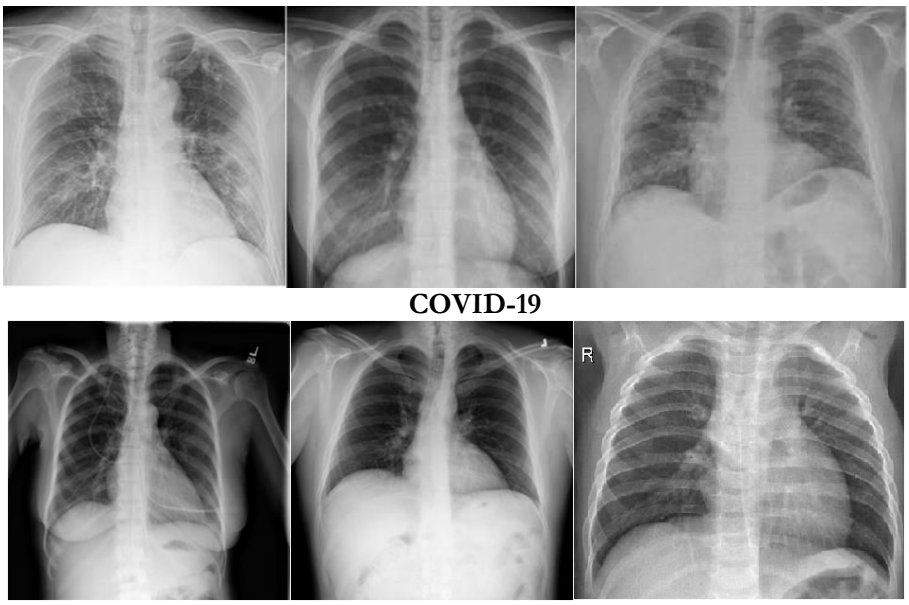

Fig. 3. Representative chest X-ray images of COVID-19 (first row), Normal (second row) patients.

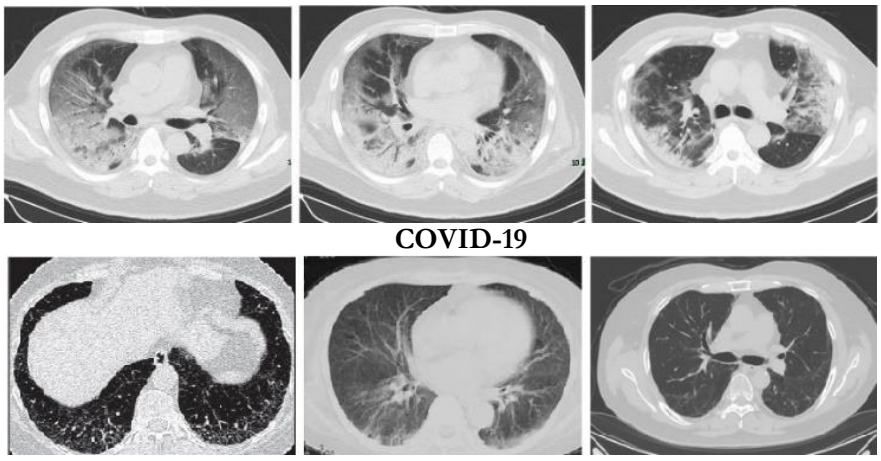

Fig. 4. Representative chest CT scan images of COVID-19 (first row), Normal (healthy) (second row) patients before transform.

2.3. Pre-trained Model

In deep learning, a convolutional neural network (CNN, or ConvNet) is a class of artificial neural networks, most commonly applied to analyze visual imagery [11]. They are also known as shift invariant or space invariant artificial neural networks (SIANN), based on the shared-weight architecture of the convolution kernels or filters that slide along input features and provide translation equivariant responses known as feature maps [12]. Counter-intuitively, most convolutional neural networks are only equivariant, as opposed to invariant, to translation [13].

The input to cov1 layer is of fixed size 224 x 224 RGB image. The image is passed through a stack of convolutional (Conv.) layers, where the filters were used with a very small receptive field: 3×3 (which is the smallest size to capture the notion of left/right, up/down, center). In one of the configurations, it also

utilizes 1×1 convolution filters, which can be seen as a linear transformation of the input channels (followed by non-linearity). The convolution stride is fixed to 1 pixel; the spatial padding of Conv. layer input is such that the spatial resolution is preserved after convolution, i.e. the padding is 1-pixel for 3×3 Conv. layers. Spatial pooling is carried out by five max-pooling layers, which follow some of the Conv. layers (not all the Conv. layers are followed by max-pooling). Max-pooling is performed over a 2×2 pixel window, with stride 2 [14]. VGG-16 model shown in Fig. 5.

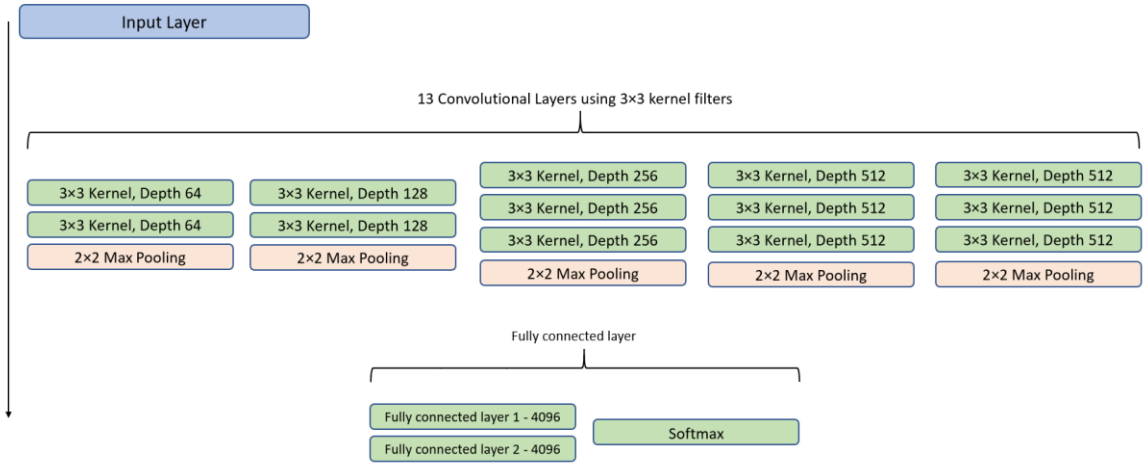

Fig. 5. VGG-16 model Architecture

Three Fully-Connected (FC) layers follow a stack of convolutional layers (which have a different depth in different architectures): the first two have 4096 channels each, the third performs 1000-way ILSVRC classification and thus contains 1000 channels (one for each class). The final layer is the soft-max layer. The configuration of the fully connected layers is the same in all networks [14]. Schematic representation of pre-trained models shown in Fig. 6.

All hidden layers are equipped with rectification (ReLU) non-linearity. It is also noted that none of the networks (except for one) contain Local Response Normalization (LRN), such normalization does not improve the performance on the ILSVRC dataset, but leads to increased memory consumption and computation time [14].

Fig. 6. Schematic representation of pre-trained models for the prediction of normal (healthy), COVID-19, bacterial, and viral pneumonia patients

3. Experimental Results

3.1. Performance evaluation measures

In the presented study, we use more than 80% of the data as the training data for training the model, the next less than 20% remaining data were used as testing data. The performance of the presented method is evaluated by using the confusion matrix. The following criteria employed for evaluation are accuracy, specificity, sensitivity, F–measure, G–mean [15] [16].

$$\text{Accuracy} = \frac{\text{TP+TN}}{\text{TP+TN+FP+FN}} \quad (1)$$

$$\text{Specifity} = \frac{\text{TP}}{\text{TN+FP}} \quad (2)$$

$$\text{Sensitivity} = \frac{\text{TP}}{\text{TP+FN}} \quad (3)$$

$$\text{F} - \text{score} = \frac{\text{2 x Precision x Recall}}{\text{Precision+Recall}} \quad (4)$$

$$\text{G} - \text{Mean} = \sqrt{\text{Sensitivity x Specifity}} \quad (5)$$

3.2. Results and Discussion

The model's set-up parameters are presented in Tabel 4. The CT Scan images after enhanced processing and scaling use the same model parameters compared to Xray.

Table 4. The configuration of the model

Parameter	X-rays Value	CT Scan Value
Batch size	128	128
Classes	3	3
Dropout	0.5	0.5
Epochs	100	100
OTP	Adam optimization	Adam optimization

To analyze the performance of the proposed method, we calculated the test accuracy, specificity, sensitivity, F–measure, and G–mean. As mentioned, the presented method has to deal with an imbalanced class distribution. The result shown in Fig.7. For this reason, accuracy cannot provide a proper performance metric and the other metrics mentioned above assess our presented model. Table 5 provides a classification result of overall (measurement with Xray model and measurement with CT-Scan model).

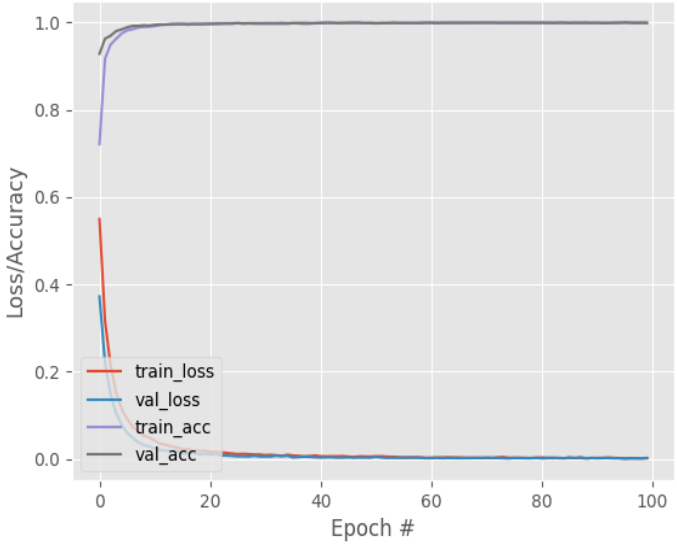

Fig. 7. Training Loss and Accuracy on COVID-19 Dataset

X-ray and CT scan data play an important role in the clinical diagnosis and also in the diagnosis of lung injury in COVID-19. Current models are built on very large databases. However, this is a case where we use the data augmentation method [17], which can partially offset the amount of dataset needed. The machine learning model is relatively accurate with Kaggle test data, continuing to check the clinical expression rate on the model's diagnoses. The data shown in Table 6 and Table 7.

Table 5. Classification results (test set)

Class	Xray_Overall	CTScan_Overall
Accuracy	0.9983	0.9987
Sensitivity	0.997	0.998
Specificity	1	1
F-score	1	1
G-Mean	0.998	0.999

Table 6. Confusion matrix of VGG16 (A test set)

X-rays Model Matrix		Predicted	
		Normal	***COVID-19***
Actual	***Normal***	24	3
	COVID-19	1	18

Table 7. Confusion matrix of VGG16 (A test set)

CT Scan Model Matrix		Predicted	
		Normal	***COVID-19***
Actual	***Normal***	22	1
	COVID-19	0	27

From the database of the Hospital in Ho Chi Minh City with medical records, conduct a 3-step check: the effectiveness of the machine learning and the patient's condition afterward. After running the model with test data from patients infected with covid-19 with different degrees and clinical manifestations, test the proportion of symptomatic patients with each of the predicted cases listed in the board. How data collect is shown in Fig. 8.

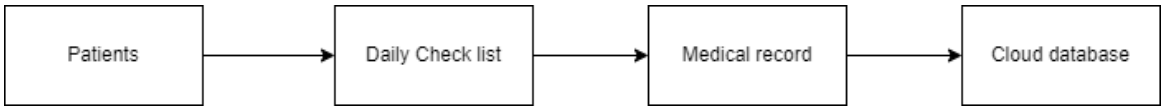

Fig. 8. Line of data collected

Data were examined across two models, followed by medical record checks of the databases used to test the percentage of extrinsic symptom characteristics for each outcome. The results show that the severity and percentage of symptoms affect the prognosis and predictive results of X-rays and CT scans through machine learning. The false prediction results show that these are mild cases with a good prognosis and little abnormal appearance on X-ray and CT scan images. The data describe in Table 8.

Table 8. Characteristics matrix of model

Matrix	**Actual**		*Y*	*Y*	*Y*	*Y*
	X-rays	*Predicted*	*Y*	*Y*	*N*	*N*
	CT scan	*Predicted*	*Y*	*N*	*Y*	*N*
	Characteristics	*Dry cough*	0.72	0.48	0.66	0.31
		Fever	0.52	0.36	0.41	0.25
		Coughing phlegm	0.46	0.28	0.4	0.22
		Sore throat	0.28	0.26	0.24	0.13
		Headache	0.19	0.12	0.14	0.011
		Diarrhea	0.06	0.02	0.02	0

4. Conclusion

Through the article, I have demonstrated the basic steps in a process of building a data-enhanced deep learning model in X-rays and CT-Scans image processing of COVID patients. The article aims to provide the most basic view, so we used the VGG-16 architecture with a modest dataset. In my actual research, I aim for some more complex and accurate architectural models such as Densenet and Resnet, along with larger data collection. Next, I may study more related application issues in CT tomography image processing of covid patients and deep learning models combined with clinical diagnoses in the

diagnosis of lung injury caused by covid. In today's clinical diagnosis, the application of deep learning is an absolute necessity when the overload and shortage of doctors is happening in some countries with underdeveloped health systems. Finding out how similar the clinical symptoms manifest together with the accuracy of deep learning models is a premise to develop applied systems that combine diagnostics, a combination of statistical analysis, and deep learning.

Acknowledgment

Thanks to the lecturers of Ho Chi Minh University of Technology for supporting this research project.

Declarations

Author contribution. All authors contributed equally to the main contributor to this paper. All authors read and approved the final paper.
Funding statement. None of the authors have received any funding or grants from any institution or funding body for the research.
Conflict of interest. The authors declare no conflict of interest.
Additional information. No additional information is available for this paper.

References

[1] S. H. Kassania, P. H. Kassanib, M. J. Wesolowskic, K. A. Schneidera, and R. Detersa, "Automatic Detection of Coronavirus Disease (COVID-19) in X-ray and CT Images: A Machine Learning Based Approach," *Biocybern Biomed Eng*, vol. 41, no. 3, pp. 867–879, Jul. 2021, doi: 10.1016/J.BBE.2021.05.013.

[2] T. P. Velavan and C. G. Meyer, "The COVID-19 epidemic," *Tropical Medicine & International Health*, vol. 25, no. 3, p. 278, Mar. 2020, doi: 10.1111/TMI.13383.

[3] J. G. Lee *et al.*, "Deep Learning in Medical Imaging: General Overview," *Korean J Radiol*, vol. 18, no. 4, pp. 570–584, May 2017, doi: 10.3348/KJR.2017.18.4.570.

[4] J. V. Shah *et al.*, "HRCT chest in COVID-19 patients: An initial experience from a private imaging center in western India," *Indian J Radiol Imaging*, vol. 31, no. Suppl 1, pp. S182–S186, Jan. 2021, doi: 10.4103/IJRI.IJRI_405_20.

[5] A. K. Jaiswal, P. Tiwari, S. Kumar, D. Gupta, A. Khanna, and J. J. P. C. Rodrigues, "Identifying pneumonia in chest X-rays: A deep learning approach," *Measurement*, vol. 145, pp. 511–518, Oct. 2019, doi: 10.1016/J.MEASUREMENT.2019.05.076.

[6] S. Bekhet, M. Hassaballah, M. A. Kenk, and M. A. Hameed, "An Artificial Intelligence Based Technique for COVID-19 Diagnosis from Chest X-Ray," *2nd Novel Intelligent and Leading Emerging Sciences Conference, NILES 2020*, pp. 191–195, Oct. 2020, doi: 10.1109/NILES50944.2020.9257930.

[7] N. Narayan Das, N. Kumar, M. Kaur, V. Kumar, and D. Singh, "Automated Deep Transfer Learning-Based Approach for Detection of COVID-19 Infection in Chest X-rays," *Ingenierie et Recherche Biomedicale*, vol. 43, no. 2, p. 114, Apr. 2022, doi: 10.1016/J.IRBM.2020.07.001.

[8] G. Gaál, B. Maga, and A. Lukács, "Attention U-Net Based Adversarial Architectures for Chest X-ray Lung Segmentation," *CEUR Workshop Proc*, vol. 2692, Mar. 2020, doi: 10.48550/arxiv.2003.10304.

[9] P. P. Shinde and S. Shah, "A Review of Machine Learning and Deep Learning Applications," *Proceedings - 2018 4th International Conference on Computing, Communication Control and Automation, ICCUBEA 2018*, Jul. 2018, doi: 10.1109/ICCUBEA.2018.8697857.

[10] K. Simonyan and A. Zisserman, "Very Deep Convolutional Networks for Large-Scale Image Recognition," *3rd International Conference on Learning Representations, ICLR 2015 - Conference Track Proceedings*, Sep. 2014, doi: 10.48550/arxiv.1409.1556.

[11] M. v. Valueva, N. N. Nagornov, P. A. Lyakhov, G. v. Valuev, and N. I. Chervyakov, "Application of the residue number system to reduce hardware costs of the convolutional neural network implementation," *Math Comput Simul*, vol. 177, pp. 232–243, Nov. 2020, doi: 10.1016/J.MATCOM.2020.04.031.

[12] K. Itoh, W. Zhang, Y. Ichioka, and J. Tanida, "Parallel distributed processing model with local space-invariant interconnections and its optical architecture," *Applied Optics, Vol. 29, Issue 32, pp. 4790-4797*, vol. 29, no. 32, pp. 4790–4797, Nov. 1990, doi: 10.1364/AO.29.004790.

[13] C. Mouton, J. C. Myburgh, and M. H. Davel, "Stride and Translation Invariance in CNNs," in *Communications in Computer and Information Science*, vol. 1342, Springer Science and Business Media Deutschland GmbH, 2020, pp. 267–281. doi: 10.1007/978-3-030-66151-9_17.

[14] C. Sitaula and M. B. Hossain, "Attention-based VGG-16 model for COVID-19 chest X-ray image classification," *Applied Intelligence*, vol. 51, no. 5, pp. 2850–2863, May 2021, doi: 10.1007/s10489-020-02055-x.

[15] M. Sokolova, N. Japkowicz, and S. Szpakowicz, "Beyond Accuracy, F-Score and ROC: A Family of Discriminant Measures for Performance Evaluation," in *AAAI Workshop - Technical Report*, vol. WS-06-06, Springer, Berlin, Heidelberg, 2006, pp. 1015–1021. doi: 10.1007/11941439_114.

[16] D. Chicco and G. Jurman, "The advantages of the Matthews correlation coefficient (MCC) over F1 score and accuracy in binary classification evaluation.," *BMC Genomics*, vol. 21, no. 1, p. 6, Jan. 2020, doi: 10.1186/s12864-019-6413-7.

[17] C. Shorten and T. M. Khoshgoftaar, "A survey on Image Data Augmentation for Deep Learning," *J Big Data*, vol. 6, no. 1, p. 60, Dec. 2019, doi: 10.1186/s40537-019-0197-0.